Accelerometer Calibration and Dynamic Bias and Gravity Estimation: Analysis, Design, and Experimental Evaluation

Pedro Batista, Carlos Silvestre, Paulo Oliveira, and Bruno Cardeira

IEEE Transactions on Control Systems Technology, vol. 19, no. 5, pp. 1128-1137, September 2011

https://doi.org/10.1109/TCST.2010.2076321

© 20XX IEEE. Personal use of this material is permitted. Permission from IEEE must be obtained for all other uses, in any current or future media, including reprinting/republishing this material for advertising or promotional purposes, creating new collective works, for resale or redistribution to servers or lists, or reuse of any copyrighted component of this work in other works.

Accepted Version

Level of access, as per info available on SHERPA/ROMEO

http://www.sherpa.ac.uk/romeo/search.php

IEEE Transactions on Control Systems Technology

Publication Information

Title	IEEE Transactions on Control Systems Technology [English]
ISSNs	Print: 1063-6536 Electronic: 1558-0865
URL	http://ieeexplore.ieee.org/xpl/RecentIssue.jsp/?punumber=87
Publishers	Institute of Electrical and Electronics Engineers [Society Publisher]

Publisher Policy

Open Access pathways permitted by this journal's policy are listed below by article version. Click on a pathway for a more detailed view.

Published Version	None, CC BY Journal Website
Accepted Version [pathway a]	None Any Repository, arXiv, Institutional Website, +3
Embargo	No Embargo
Copyright Owner	Publishers
Location	Any Repository Author's Homepage Institutional Repository Institutional Website Named Repository (arXiv, TechRxiv)
Conditions	When accepted for publication, set statement to accompany deposit (see policy) Must link to publisher version with DOI Publisher copyright and source must be acknowledged
Accepted Version [pathway b]	24m arXiv, Funder Designated Location, Institutional Website
Submitted Version [pathway a]	None arXiv, Funder Designated Location, TechRxiv, +3
Submitted Version [pathway b]	None Academic Social Network

For more information, please see the following links:

- IEEE Copyright Policy
- Section 8.1.9 of the PSPB Operations Manual
- Policy: Posting Your Article
- IEEE Open
- Author Posting of IEEE Copyrighted Papers Online
- Electronic IEEE Copyright Form

Accelerometer Calibration and Dynamic Bias and Gravity Estimation: Analysis, Design, and Experimental Evaluation

Pedro Batista, *Student Member, IEEE,* Carlos Silvestre, *Member, IEEE,* Paulo Oliveira *Member, IEEE,* and Bruno Cardeira, *Member, IEEE*

***Abstract*—Tri-axial linear accelerometers are key components in a great variety of applications and, in particular, in navigation systems. Nonidealities such as scale factors, cross coupling, bias, and other higher-order nonlinearities affect the output of this sensor, leading, in general, to prohibitive errors. On the other hand, these coefficients are often time-varying, which renders off-line calibration less effective. One such coefficient that usually varies greatly over time and between power-ons is the bias. This paper details the calibration of an accelerometer unit and presents also a dynamic filtering solution for the bias, which also includes the estimation of the gravity in body-fixed coordinates. Simulation and experimental results obtained with a Motion Rate Table are presented and discussed to illustrate the performance of the proposed algorithms.**

I. Introduction

RECENT advances in materials and production processes have led to the increasingly miniaturization of a large variety of sensing devices. Among these sensors are a new generation of Micro Electro-Mechanical Systems (MEMS) accelerometers, which are nowadays used in a large variety of applications. These sensors have good dynamic specifications, considering the cost, size, and power requirements, but are often subject to large offsets, cross-coupling factors, and other nonlinearities. While in some cases these nonidealities are of no importance, e.g. in cell phones to detect the vertical direction or in computer hardware for active hard drive protection, they are prohibitive for the design of navigation systems, which justifies off-line calibration. Furthermore, the coefficients of these nonidealities are often time-varying, which renders off-line calibration less effective and substantiates the need for on-line parameter estimation. This paper presents the calibration of a low-cost triaxial accelerometer and a novel filtering solution for on-line bias and gravity estimation with application to the design of navigation systems for mobile platforms.

High performance accelerometers are a key element and have been extensively used in Inertial Navigation Systems (INS). With the widespread use of MEMS technology, accelerometers are nowadays a fundamental aiding sensor for attitude estimation in low-cost, middle range performance Attitude and Heading Reference Systems (AHRS), with application to autonomous air, ground, and ocean robots. These inexpensive, low power sensors, used as pendula, allow for accurate attitude estimates at very low frequency by comparing the Earth gravitational field vector measurements in body frame coordinates with the vertical, see [1], [2], and references therein for examples of such application in attitude estimation. The integration of accelerometer readings with GPS measurements are commonly employed for linear motion estimation in Integrated Navigation Systems, see [3] and references therein for examples of such application.

The topic of accelerometer calibration has been subject of intensive research. Indeed, various methods have been proposed in the literature, from precision centrifuge tests of linear accelerometers [4] to multi-position methods [5] [6] [7]. In [8], error models for inertial sensors, including a solid-state triaxial accelerometer, were explicitly included in an Extended Kalman Filter (EKF) to estimate the position and orientation of a robot, while in [9] Kalman filtering techniques were applied to the calibration and alignment of Inertial Navigation Systems, which was also studied in [10]. More recently, in [11], nonlinear Kalman filters, of first and second order, coupled with position feedback, were used to characterize accelerometers. An optimization-based calibration procedure for triaxial accelerometer-magnetometers was proposed in [12], where a robotic arm is used to generate different angular positions of the body of the sensor. In [13] a fully electrical setup was proposed to test and calibrate accelerometer MEMS sensors and a case study was presented in [14], where a 4-DOF system is proposed for fully automated accelerometer calibration. An interesting survey on the history of accelerometers, which also includes a section on calibration activities, is found in [15].

The contribution of the paper is twofold: i) an accelerometer calibration technique is proposed and applied to off-line accelerometer calibration that includes the estimation of bias, scale factors, cross coupling factors, and quadratic coefficients; ii) a time-varying Kalman filter is derived for on-line dynamic bias and gravity estimation. The calibration technique proposed in the paper resorts to attitude relative measurements as provided by a Motion Rate Table (MRT). The a priori knowledge of the gravity vector is not required

This work was partially supported by Fundação para a Ciência e a Tecnologia (ISR/IST plurianual funding), by the projects PTDC/EEAACR/72853/2006 HELICIM and PTDC/MAR/64546/2006 - OBSERVFLY of the FCT, and by the AIRTICI project from AdI.

The work of P. Batista was supported by a PhD Student Scholarship from the POCTI Programme of FCT, SFRH/BD/24862/2005.

The authors are with the Institute for Systems and Robotics, Instituto Superior Técnico, Av. Rovisco Pais, 1049-001 Lisboa, Portugal. {pbatista,cjs,pjcro,bcardeira}@isr.ist.utl.pt

since it is also explicitly estimated, in contrast with previous methods that assume that the vertical is known. The second part of paper is of particular importance for the design of navigation systems since it allows for online estimation of the accelerometer bias which, for low-cost units, is usually time-varying, rendering off-line calibration less effective. Moreover, the gravity is also estimated, in body-fixed coordinates. This is in contrast with previous solutions where the gravitational term is canceled resorting to the knowledge of the attitude of the body, therefore leading to cancellation problems that lead to a severe degradation in the performance of the resulting navigation systems. In addition to simulation results, the proposed algorithms were experimentally evaluated resorting to a motion rate table, which offers ground truth data.

The paper is organized as follows. The accelerometer models are presented and discussed in Section II. Section III details the off-line calibration technique proposed in the paper, while the on-line dynamic bias and gravity estimation solution is derived in Section IV. Simulation and experimental results are given in Sections V and VI, respectively, including both the off-line calibration of a low-cost MEMS accelerometer and dynamic bias and gravity estimation tests. Finally, Section VII summarizes the main conclusions and contributions of the paper.

A. Notation

Throughout the paper the symbol $\mathbf{0}$ denotes a matrix of zeros and $\mathbf{I}$ an identity matrix, both of appropriate dimensions, while $\mathrm{diag}(\mathbf{A}_1, \ldots, \mathbf{A}_\mathrm{n})$ is a block diagonal matrix. If $\mathbf{x}$ and $\mathbf{y}$ are two vectors of identical dimensions, $\mathbf{x} \times \mathbf{y}$ represent the cross products. For $\mathbf{x} = [x_1 \ \ldots x_n]^T \in \mathbb{R}^n$, the vector $\boldsymbol{x}^i$ is defined as the vector that results of the element-wise power operation, i.e., $\mathbf{x}^i := \left[x_1^i \ \ldots x_n^i\right]^T \in \mathbb{R}^n$, while the vector $\boldsymbol{x}^{|i|}$ is defined as

$$\boldsymbol{x}^{|i|} := \begin{bmatrix} \mathrm{sign}\,(\mathrm{x_1})\,\mathrm{x_1^i} \\ \vdots \\ \mathrm{sign}\,(\mathrm{x_n})\,\mathrm{x_n^i} \end{bmatrix}.$$

The rotation matrix from a coordinate frame $\{A\}$ to a coordinate frame $\{B\}$ is denoted by ${}^B_A\mathbf{R}$. Finally, the Dirac delta function is denoted by $\delta(t)$.

II. Accelerometer Model

The simplest accelerometer model for single axis sensors considers only a scale factor and a constant offset, as given by

$$a_m(t) = fa(t) + b,$$

where a_m is the output of the accelerometer, f is the scale factor, b denotes the bias, and $a(t)$ stands for the acceleration that is measured in the absence of offsets, which includes not only the acceleration of the body of the accelerometer but also a term due to the effect of the gravitational field on the mass whose acceleration is actually measured, which is not coincident with the accelerometer case. Notice that the term due to the gravitational field appears regardless of the accelerometer technology as all objects are subject to the gravitational force, which induces a force of opposite direction to the gravity on the mass whose acceleration is actually measured, see [5] and [16] for further details.

For navigation purposes, tri-axial accelerometers, composed of three, single-axis, orthogonally mounted linear accelerometers, are employed. The generalization of the simplest single-axis model for tri-axial accelerometers, which accounts for scale factors and bias, reads as

$$\mathbf{a}_m(t) = \mathbf{F}\mathbf{a}(t) + \mathbf{b}, \tag{1}$$

where $\mathbf{F} \in \mathbb{R}^{3\times3}$ is a diagonal matrix that includes the scale factors, $\mathbf{b} \in \mathbb{R}^3$ is the bias, and

$$\mathbf{a}(t) = \dot{\mathbf{v}}(t) + \mathbf{S}\left[\boldsymbol{\omega}(t)\right]\mathbf{v}(t) - \mathbf{g}(t),$$

where $\mathbf{v}$ and $\boldsymbol{\omega}$ denote the linear and angular velocities of the body-fixed frame $\{B\}$, respectively, expressed in body-frame coordinates, $\mathbf{S}\left[\boldsymbol{\omega}(t)\right] \in \mathbb{R}^{3\times3}$ is the skew symmetric matrix such that $\mathbf{S}\left[\boldsymbol{\omega}(t)\right]\mathbf{v}(t) = \boldsymbol{\omega}(t) \times \mathbf{v}(t)$, and $\mathbf{g}(t) \in \mathbb{R}^3$ is the acceleration of gravity, expressed in body-fixed coordinates. In practice, the set of single-axis accelerometers is not orthogonally mounted, which introduces cross coupling between the acceleration felt on the different accelerometer axes. This nonideality may be simply modeled by no longer considering $\mathbf{F}$ as a diagonal matrix. Instead, $\mathbf{F}$ is just assumed to be an invertible matrix, which accounts simultaneously, in this case, for scale and cross coupling factors.

The accelerometer model (1) is still, and in spite of capturing already a different number of nonidealities, only an approximation of the real model. Indeed, the electrical devices involved in the measurement process, from transducers to amplifiers, are not linear, do not have constant coefficients, and are subject to different types of noise. A more complete (and complex) model [4], that includes higher-order terms, is given by

$$\begin{aligned}\mathbf{a}_m(t) = \mathbf{F}\mathbf{a}(t) + \mathbf{b} + \mathbf{F}\mathbf{F}_2\mathbf{a}^2(t) + \mathbf{F}_{|2|}\mathbf{a}^{|2|}(t) \\ + \mathbf{F}\mathbf{F}_3\mathbf{a}^3(t) + \mathbf{F}\mathbf{F}_{|3|}\mathbf{a}^{|3|}(t) + \ldots\end{aligned}$$

where $\mathbf{F}_2 \in \mathbb{R}^{3\times3}$, $\mathbf{F}_{|2|} \in \mathbb{R}^{3\times3}$, $\mathbf{F}_3 \in \mathbb{R}^{3\times3}$, and $\mathbf{F}_{|3|} \in \mathbb{R}^{3\times3}$ are diagonal matrices.

Nonlinear time-varying models for accelerometers, with many parameters, offer better accuracies, at the expense of the complexity. From the practical point of view, it seems appealing to use simpler methods that preserve accuracy as: i) for very highly nonlinear time-varying dynamic models the complexity of the inversion of the model could be overwhelming. Closed-form solutions are obviously not available and iterative numerical solvers would be required to operate in real-time; ii) time-varying models would be likely to depend on other variables such as temperature, which would require additional sensors; and iii) the effect of higher-order nonlinearities is often very mild, particularly when compared to the magnitude of the electrical noise. Therefore, the model employed in this work, and after successful experimental validation of the model accuracy, is

$$\mathbf{a}_m(t) = \mathbf{F}\left[\mathbf{a}(t) + \mathbf{F}_2\mathbf{a}^2(t)\right] + \mathbf{b} + \mathbf{n}_a(t), \tag{2}$$

where $\mathbf{n}_a(t)$ denotes the accelerometer noise. The quadratic even term was chosen as it was evident, from experimental

evaluation, that this was the most dominant nonlinear term. Moreover, there exists a closed-form solution to obtain $\mathbf{a}(t)$ from (2), which is a precious advantage for real-time navigation applications since no iterative solvers are required.

III. Accelerometer Off-line Calibration

There exists a multitude of tests and calibration procedures described in the literature. In this paper it is assumed that the accelerometer is exposed to several different known rotations and a rather large number of measurements is taken at each static position. This can be achieved resorting to a tri-axial motion rate table, e.g., the Ideal Aerosmith Model 2103HT, used in this work to obtain the experimental data.

The motion rate table outputs the rotation from body-fixed to inertial coordinates apart from an installation error due to non-horizontal mounting of the table. If there is a precision level available, this installation error is known and it is possible to compute the rotation matrix $\mathbf{R}$ from body-fixed to inertial coordinates. Otherwise, it is necessary to consider

$$\mathbf{R}(t) = {}^{I}_{T}\mathbf{R}\ {}^{T}_{B}\mathbf{R}\,(t)$$

where ${}^{T}_{B}\mathbf{R}$ is the rotation from body-fixed coordinates to the table installation fixed reference frame, which is given by the calibration table, and ${}^{I}_{T}\mathbf{R}$ corresponds to the matrix that encodes the installation offset.

Since measurements are considered only at static positions, it is true that

$$\mathbf{v}(t) = \dot{\mathbf{v}}(t) = \mathbf{0}.$$

Therefore, using (2), the nominal accelerometer readings are given by

$$\mathbf{a}_m(t) = \mathbf{F}\left[-\mathbf{g}(t) + \mathbf{F}_2\mathbf{g}^2(t)\right] + \mathbf{b}. \tag{3}$$

The acceleration of gravity in body-fixed coordinates may be expressed as

$$\mathbf{g}(t) = \mathbf{R}^T(t)\,{}^{I}\mathbf{g},$$

where ${}^{I}\mathbf{g}$ is the acceleration of gravity expressed in inertial coordinates. Nowadays, there exist very accurate models for the acceleration of the gravity, e.g., using the 1984 World Geodetic System (WGS84), see [17] for further details. Therefore, if $\mathbf{R}$ is known, the computation of $\mathbf{F}$, $\mathbf{F}_2$, and $\mathbf{b}$ corresponds to the simple determination of linear coefficients. In the case considered in the paper only ${}^{T}_{B}\mathbf{R}$ is known, which means that the direction of the gravity must also be determined. In this case, it is possible to rewrite (3) as

$$\mathbf{a}_m(t) = \mathbf{F}\left(-\,{}^{T}_{B}\mathbf{R}^{\,T}(t){}^{T}\mathbf{g} + \mathbf{F}_2\left[{}^{T}_{B}\mathbf{R}^{\,T}(t)\,{}^{T}\mathbf{g}\right]^2\right) + \mathbf{b}, \tag{4}$$

where

$${}^{T}\mathbf{g} = {}^{I}_{T}\mathbf{R}^{T}\,{}^{I}\mathbf{g}$$

is the acceleration of gravity expressed in table-fixed coordinates. Multiplying (4) on the left by $\mathbf{F}^{-1}$ gives

$$\mathbf{F}^{-1}\mathbf{a}_m(t) + {}^{T}_{B}\mathbf{R}^{\,T}(t)\,{}^{T}\mathbf{g} - \mathbf{F}_2\left[{}^{T}_{B}\mathbf{R}^{\,T}(t)\,{}^{T}\mathbf{g}\right]^2 - \mathbf{b}' = \mathbf{0}, \tag{5}$$

where

$$\mathbf{b}' = \mathbf{F}^{-1}\mathbf{b}.$$

Equation (5) presents a better form than (4) in order to estimate the unknown parameters $\mathbf{F}$, $\mathbf{b}$, $\mathbf{F}_2$, and the acceleration of gravity in table coordinates, ${}^{T}\mathbf{g}$, since it has less products between unknowns. Nevertheless, a quadratic term still exists. In the presence of noise, there is no exact solution to (5) if a large set of measurements is considered. A simple and computationally efficient way to calibrate the accelerometer is to solve an optimization problem in two steps. First, the quadratic term is ignored, which allows to write, for a set of static measurements $\{\mathbf{a}_m(t_i), i = 1, \ldots, N\}$, corresponding to a set of rotation matrices $\{{}^{T}_{B}\mathbf{R}\,(t_i), i = 1, \ldots, N\}$,

$$\begin{bmatrix} \mathbf{D}_a(t_i) & {}^{T}_{B}\mathbf{R}^{\,T}(t_i) & -\mathbf{I} \end{bmatrix} \begin{bmatrix} \mathbf{f} \\ {}^{T}\mathbf{g} \\ \mathbf{b} \end{bmatrix} = \mathbf{0},$$

where

$$\mathbf{D}_a(t) = \begin{bmatrix} \mathbf{a}_m^T(t) & \mathbf{0} & \mathbf{0} \\ \mathbf{0} & \mathbf{a}_m^T(t) & \mathbf{0} \\ \mathbf{0} & \mathbf{0} & \mathbf{a}_m^T(t) \end{bmatrix} \in \mathbb{R}^{3\times 9}$$

and

$$\mathbf{f} = \begin{bmatrix} \mathbf{f}_1 \\ \mathbf{f}_2 \\ \mathbf{f}_3 \end{bmatrix} \in \mathbb{R}^9,\ \mathbf{F}^{-1} = \begin{bmatrix} \mathbf{f}_1^T \\ \mathbf{f}_2^T \\ \mathbf{f}_3^T \end{bmatrix}.$$

In the presence of sensor noise a simple solution is easily obtained from the vector associated with the minimum singular value of the Singular Value Decomposition (SVD) of the stack matrix

$$\mathbf{X} = \begin{bmatrix} \mathbf{D}_a(t_1) & {}^{T}_{B}\mathbf{R}^{\,T}(t_1) & -\mathbf{I} \\ \mathbf{D}_a(t_2) & {}^{T}_{B}\mathbf{R}^{\,T}(t_2) & -\mathbf{I} \\ \vdots & \vdots & \vdots \\ \mathbf{D}_a(t_N) & {}^{T}_{B}\mathbf{R}^{\,T}(t_N) & -\mathbf{I} \end{bmatrix}.$$

The magnitude of the acceleration of gravity, as well as its direction, are used to normalize the resulting SVD solution.

The solution of this first step, in particular the gravity vector, is used as an estimate for the quadratic term in (5), which allows to also consider (5) as linear in the parameters, with

$$\left[\mathbf{D}_a(t_i)\ \ {}^{T}_{B}\mathbf{R}^{T}(t_i)\ \ -\mathrm{diag}\left(\left[{}^{T}_{B}\mathbf{R}^{T}(t_i)\ {}^{T}\hat{\mathbf{g}}\right]^2\right)\ \ -\mathbf{I}\right] \begin{bmatrix} \mathbf{f} \\ {}^{T}\mathbf{g} \\ \mathbf{f}_2 \\ \mathbf{b} \end{bmatrix} = \mathbf{0},$$

where $\mathbf{f}_2 \in \mathbb{R}^3$ is the vector that contains the diagonal elements of the diagonal matrix $\mathbf{F}_2$ and ${}^{T}\hat{\mathbf{g}}$ is the estimate of the gravity vector previously obtained. Stacking all observations gives

$$\mathbf{X}_2 \begin{bmatrix} \mathbf{f} \\ {}^{T}\mathbf{g} \\ \mathbf{f}_2 \\ \mathbf{b} \end{bmatrix} = \mathbf{0},$$

with

$$\mathbf{X}_2 = \begin{bmatrix} \mathbf{D}_a(t_1) & {}^{T}_{B}\mathbf{R}^{\,T}(t_1) & -\mathrm{diag}\left(\left[{}^{T}_{B}\mathbf{R}^{T}(t_1)\ {}^{T}\hat{\mathbf{g}}\right]^2\right) & -\mathbf{I} \\ \mathbf{D}_a(t_2) & {}^{T}_{B}\mathbf{R}^{\,T}(t_2) & -\mathrm{diag}\left(\left[{}^{T}_{B}\mathbf{R}^{T}(t_2)\ {}^{T}\hat{\mathbf{g}}\right]^2\right) & -\mathbf{I} \\ \vdots & \vdots & \vdots & \\ \mathbf{D}_a(t_N) & {}^{T}_{B}\mathbf{R}^{\,T}(t_N) & -\mathrm{diag}\left(\left[{}^{T}_{B}\mathbf{R}^{T}(t_N)\ {}^{T}\hat{\mathbf{g}}\right]^2\right) & -\mathbf{I} \end{bmatrix}.$$

TABLE I
ALGORITHM TO CALIBRATE THE ACCELEROMETER

1) Compute the SVD of $\mathbf{X}$. Select the vector associated with the minimum singular value.
2) Normalize the SVD solution obtained in Step 1 according to the magnitude of the gravity and its direction (sign of the z-coordinate).
3) Use the gravity estimate obtained in Step 2 and compute the SVD of $\mathbf{X}_2$. Select the vector associated with the minimum singular value.
4) Normalize the SVD solution obtained in Step 3 according to the magnitude of the gravity and its direction (sign of the z-coordinate).
5) Use the current gravity estimate in $\mathbf{X}_2$ and go to Step 3. Stop once the difference between the previous gravity estimate and the most recent goes below a predefined threshold.

The parameters are readily obtained by computing the vector associated with the minimum singular value of $\mathbf{X}_2$ and normalizing it according to the known magnitude of the gravity. Finally, it is possible to reiterate this last step using as new gravity estimate the solution of each previous step. The proposed algorithm is detailed in Table I.

IV. Dynamic Bias and Gravity Estimation

Although theoretically possible for certain maneuvers, online estimation of the parameters of the accelerometer model (2) is not practical: the number of unknown coefficients is too large and highly aggressive maneuvers would be required to achieve only a moderate performance. However, it is important to include, in navigation systems, a simplified model to account for some of the nonidealities of the accelerometers. The simplest of these is the sensor bias, and while it is only one constant for each axis, it is well known that an offset in the acceleration measurement results in a severe degradation of the performance of navigation solutions. Furthermore, experimental results evidence that this parameter varies greatly, not only over time but also between power-ons.

It was shown in [18] that, assuming that the accelerometer has been previously calibrated, removing the effect of scale and cross factor errors and ignoring higher-order nonlinearities, the bias may be estimated under some mild assumptions. Therefore, it is assumed in this section that the accelerometer has been previously calibrated using the technique proposed in the previous section, which allows to use the model

$$\mathbf{a}_m(t) = \dot{\mathbf{v}}(t) + \mathbf{S}\left[\boldsymbol{\omega}(t)\right]\mathbf{v}(t) - \mathbf{g}(t) + \mathbf{b} + \mathbf{n}_a(t). \quad (6)$$

The acceleration of gravity $\mathbf{g}$ is not known in robotic applications. While there are models for its magnitude, its direction depends on the attitude of the robot, and it is used, in fact, to estimate this variable. A common assumption when designing attitude filters is that the magnitude of the acceleration of gravity dominates, for sufficiently low frequencies, the other terms, see [1] for an example of such application. The direction of the gravity is approximated, in that case, by

$$\mathbf{d}_{\mathbf{g}} \approx \frac{\mathbf{a}_m(t)}{\|\mathbf{a}_m(t)\|},$$

which induces errors in the attitude estimates. While these errors are in general negligible, they may prove to be prohibitive for highly maneuvering vehicles, e.g. aerial robots, vehicles executing trajectories with approximately constant accelerations, or applications where high-accuracy requirements are in place, such as space applications. Therefore, the gravity acceleration in body-coordinates is also considered as an unknown in this framework.

The direction of the acceleration of gravity is locally constant in inertial coordinates. Therefore, the time derivative of $\mathbf{g}$ is simply given by

$$\dot{\mathbf{g}}(t) = -\mathbf{S}\left[\boldsymbol{\omega}(t)\right]\mathbf{g}(t).$$

The bias is assumed to be constant, which means that

$$\dot{\mathbf{b}}(t) = \mathbf{0}.$$

Finally, from (6), it is possible to write

$$\dot{\mathbf{v}}(t) = \mathbf{a}_m(t) - \mathbf{S}\left[\boldsymbol{\omega}(t)\right]\mathbf{v}(t) + \mathbf{g}(t) - \mathbf{b} - \mathbf{n}_a(t).$$

In the present work it is assumed that linear velocity readings are available in order to estimate $\mathbf{b}$ and $\mathbf{g}$. Nevertheless, extending the framework to also estimate $\mathbf{v}$ considering linear position measurements is trivial, see [18] for further details. The final system dynamics, considering state disturbances and measurement noise, are given by

$$\begin{cases} \dot{\mathbf{x}}(t) = \mathbf{A}(t)\mathbf{x}(t) + \mathbf{B}\mathbf{a}_m(t) + \mathbf{n}_x(t) \\ \mathbf{y}(t) = \mathbf{C}\mathbf{x}(t) + \mathbf{n}_y(t) \end{cases}, \quad (7)$$

where $\mathbf{x}(t) = \left[\mathbf{v}^T(t)\ \mathbf{g}^T(t)\ \mathbf{b}^T(t)\right]^T$ is the system state,

$$\mathbf{A}(t) = \begin{bmatrix} -\mathbf{S}\left[\boldsymbol{\omega}(t)\right] & \mathbf{I} & -\mathbf{I} \\ \mathbf{0} & -\mathbf{S}\left[\boldsymbol{\omega}(t)\right] & \mathbf{0} \\ \mathbf{0} & \mathbf{0} & \mathbf{0} \end{bmatrix},$$

$$\mathbf{B} = \begin{bmatrix} \mathbf{I} \\ \mathbf{0} \\ \mathbf{0} \end{bmatrix},$$

$\mathbf{C} = [\mathbf{I}\ \mathbf{0}\ \mathbf{0}]$, and $\mathbf{n}_x$ and $\mathbf{n}_y$ are assumed to be zero-mean white Gaussian noise, with

$$\mathrm{E}\left[\mathbf{n}_{\mathrm{x}}\left(\mathrm{t}_1\right)\mathbf{n}_{\mathrm{x}}^{\mathrm{T}}\left(\mathrm{t}_2\right)\right] = \boldsymbol{\Xi}\delta\left(\mathrm{t}_1 - \mathrm{t}_2\right),$$

$$\mathrm{E}\left[\mathbf{n}_{\mathrm{y}}\left(\mathrm{t}_1\right)\mathbf{n}_{\mathrm{y}}^{\mathrm{T}}\left(\mathrm{t}_2\right)\right] = \boldsymbol{\Theta}\delta\left(\mathrm{t}_1 - \mathrm{t}_2\right),$$

and

$$\mathrm{E}\left[\mathbf{n}_{\mathrm{x}}\left(\mathrm{t}_1\right)\mathbf{n}_{\mathrm{y}}^{\mathrm{T}}\left(\mathrm{t}_2\right)\right] = \mathbf{0},$$

where $\boldsymbol{\Xi}$ and $\boldsymbol{\Theta}$ are the process and noise intensity matrices, respectively. The linear time-varying system (7) is observable on $[t_0, t_f]$ if and only if the direction of the angular velocity $\boldsymbol{\omega}(t)$ changes for some $t_1 \in [t_0, t_f]$ or, equivalently,

$$\underset{\substack{\mathbf{d} \in \mathbb{R}^3 \\ \|\mathbf{d}\| = 1.}}{\forall} \quad \underset{t_1 \in [t_0, t_f]}{\exists} \quad : \quad \mathbf{S}\left[\boldsymbol{\omega}\left(t_1\right)\right]\mathbf{d} \neq \mathbf{0}.$$

The proof of this result can be found in [18]. Therefore, the estimation problem is well-posed and the time-varying Kalman filter design is straightforward, see [19] and [20]. For the sake of completeness, the Kalman filter equations are given by

$$\dot{\hat{\mathbf{x}}}\left(t\right) = \mathbf{A}(t)\hat{\mathbf{x}}\left(t\right) + \mathbf{K}\left(t\right)\left[\mathbf{y}\left(t\right) - \mathbf{C}\hat{\mathbf{x}}\left(t\right)\right]$$

for the state estimate, while the covariance matrix evolves according to

$$\dot{\mathbf{P}}(t) = \mathbf{A}\left(t\right)\mathbf{P}(t) + \mathbf{P}(t)\,\mathbf{A}\left(t\right) + \boldsymbol{\Xi}(t) - \mathbf{P}(t)\,\mathbf{C}^T\boldsymbol{\Theta}^{-1}\mathbf{C}\mathbf{P}(t).$$

The Kalman gain matrix is given by

$$\mathbf{K}(t) = \mathbf{P}(t)\,\mathbf{C}^T\mathbf{\Theta}^{-1}(t).$$

Remark 1: Notice that, even though the nominal system considers $\dot{\mathbf{b}}(t) = 0$, in the filter design the bias is assumed to be driven by zero mean, white Gaussian noise. This allows the filter to track slowly time-varying bias, in addition to variations between power-ons. The intensity of the white noise that is assumed to drive the bias is a parameters that can be selected according to the change rate of the bias.

V. Simulation Results

This section presents simulation results that were carried out prior to the experimental tests in order to assess the performance of the proposed solutions. The simulations attempt to replicate the experimental trials so that the results are comparable. The multi-position accelerometer calibration algorithm is evaluated in Section V-A, while simulation results with the proposed filtering solution for dynamic bias and gravity estimation are presented in Section V-B.

A. Accelerometer Calibration

In order to assess the effectiveness of the proposed calibration method, Monte Carlo simulations were first carried out considering an accelerometer with

$$\mathbf{F}^{-1} = \begin{bmatrix} 0.990 & 0.001 & -0.002 \\ 0.020 & 1.005 & 0.003 \\ -0.010 & -0.004 & 1.010 \end{bmatrix},$$

$$\mathbf{b}' = \begin{bmatrix} 0.05 \\ -0.01 \\ 0.04 \end{bmatrix} (\mathrm{m/s^2}),$$

and

$$\mathbf{F}_2 = 10^{-4}\mathrm{diag}\left(2.5, 1.5, -0.75\right).$$

In addition to that, sensor noise was considered. In particular, zero-mean additive white Gaussian noise was added to the acceleration measurements, with standard deviation of $0.0013\,\mathrm{m/s^2}$. In each simulation the attitude of the accelerometer varies according to Fig. 1, where the evolution of the roll, pitch, and yaw Euler angles is depicted. The corresponding evolution of the resulting gravity vector is shown in Fig. 2. As it is possible to observe, the attitude trajectory evolves in steps and covers many different configurations, not only to have the calibration problem well-posed (sufficient data) but also to achieve better results. A transition time of $2\,\mathrm{s}$ is used between steps and each step lasts $22\,\mathrm{s}$. The data is sampled, at a sampling rate of $100\,\mathrm{Hz}$, during a period of $4\,\mathrm{s}$ on each step, in which the accelerometer is static, for calibration purposes. The first and last periods of $180\,\mathrm{s}$ of the simulation are presented solely because they will be required for hardware synchronization purposes.

The resulting mean of the errors of the estimated parameters is below 10^{-9} for all variables, which evidences that the estimates are unbiased. On the other hand, the standard deviation of the error stays below 10^{-7}, which corresponds to very accurate estimates of the accelerometer parameters. These values show that the proposed calibration procedure should yield good results in practice.

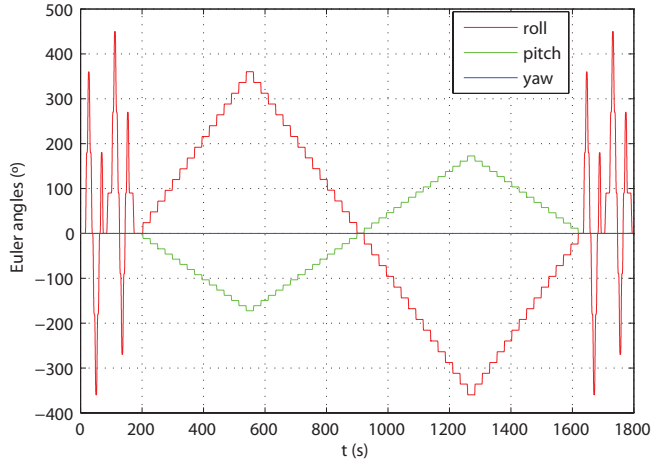

Fig. 1. Evolution of the Euler angles for accelerometer calibration

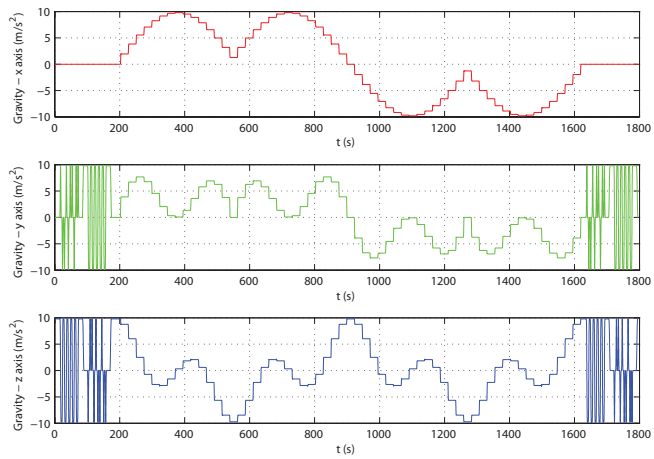

Fig. 2. Evolution of the gravity (expressed in body-fixed coordinates)

B. Dynamic Bias and Gravity Estimation

In order to evaluate the performance of the proposed bias and gravity estimation solution, simulations were carried out considering a setup very similar to the experimental one, which will be presented in the following section. In particular, the rotation of the accelerometer is parameterized by roll, pitch, and yaw Euler angles, whose evolution is depicted in Fig. 3.

Additive zero-mean white Gaussian noise was considered for all sensors, which were sampled at 100Hz. The standard deviations were chosen as $0.0013\,\mathrm{m/s^2}$ for the acceleration measurements, 0.05 °/s for the angular velocity readings, and $0.01\,\mathrm{m/s}$ for the linear velocity measurements. In addition, the bias of the accelerometer was set to

$$\mathbf{b}' = \begin{bmatrix} 0.1 \\ -0.05 \\ 0.025 \end{bmatrix} (\mathrm{m/s^2}).$$

The filter parameters were chosen as

$$\mathbf{\Xi} = \mathrm{diag}\left(10^{-3}\mathbf{I}, 10^{-4}\mathbf{I}, 10^{-5}\mathbf{I}\right)$$

and

$$\mathbf{\Theta} = 0.1\mathbf{I}.$$

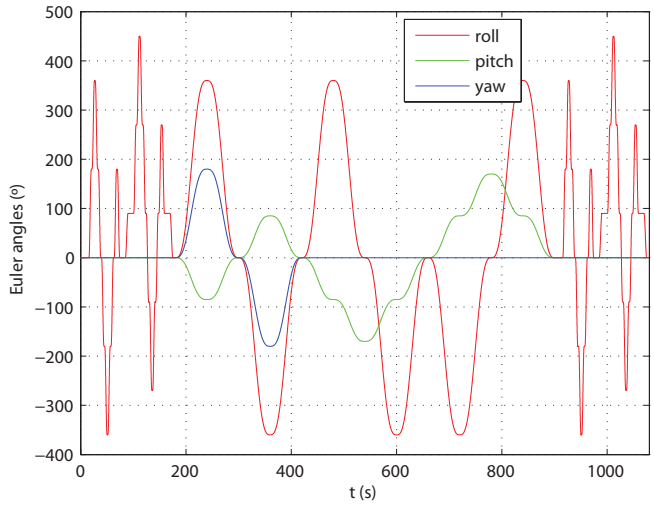

Fig. 3. Evolution of the Euler angles for dynamic bias and gravity estimation

Finally, the initial velocity and gravity estimates were set close to the true values, as the velocity is measured and the acceleration of gravity is known up to some error (the acceleration measurement is dominated by the gravity). The initial bias estimate was set to zero.

The evolution of the gravity and bias estimates are depicted in Figs. 4 and 5, respectively. As it is possible to observe, the

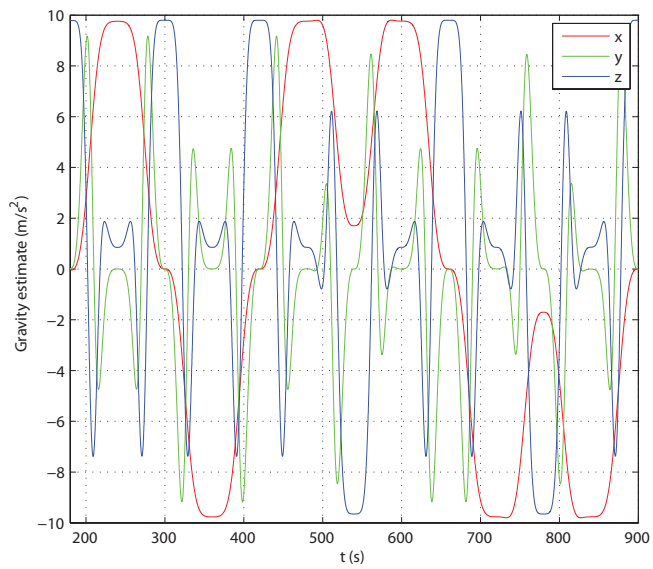

Fig. 4. Evolution of the gravity estimate (in body-fixed coordinates)

bias converges quickly to the true values. In order to better evaluate the performance of the filter, the evolution of the errors of the linear velocity, gravity, and bias are depicted in Figs. 6, 7, and 8, respectively. Clearly, the mean errors converge to zero. Moreover, the errors on the bias and gravity estimates stay well below the noise of the accelerometer, which evidences good filtering performance of the proposed solutions.

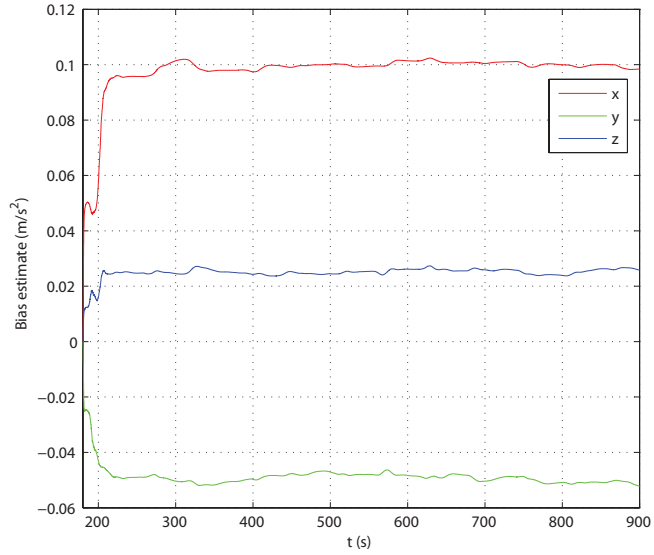

Fig. 5. Evolution of the bias estimate

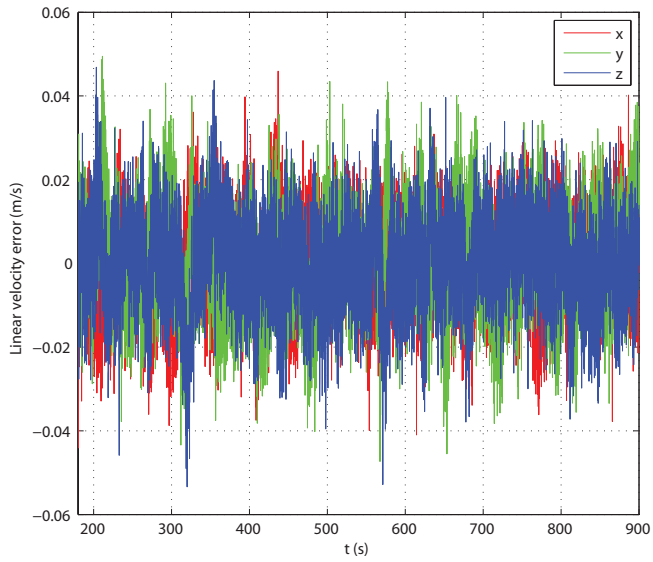

Fig. 6. Evolution of the linear velocity error

VI. Experimental Evaluation

Experimental results were carried out in order to evaluate the performance of the proposed solutions. The experimental setup is detailed in Section VI-A, while the accelerometer calibration procedure and results are presented in Section VI-B. Finally, the proposed filtering solution for dynamic bias and gravity estimation is analyzed in Section VI-C.

A. Experimental Setup

To obtain high quality results, a calibration procedure requires the execution of specific maneuvers, involving the acquisition of high accuracy ground truth data to evaluate the estimated quantities produced by processing accelerometer data. The Model 2103HT from Ideal Aerosmith [21] is a three-axis MRT that provides precise angular position, rate and acceleration for development and testing of inertial components

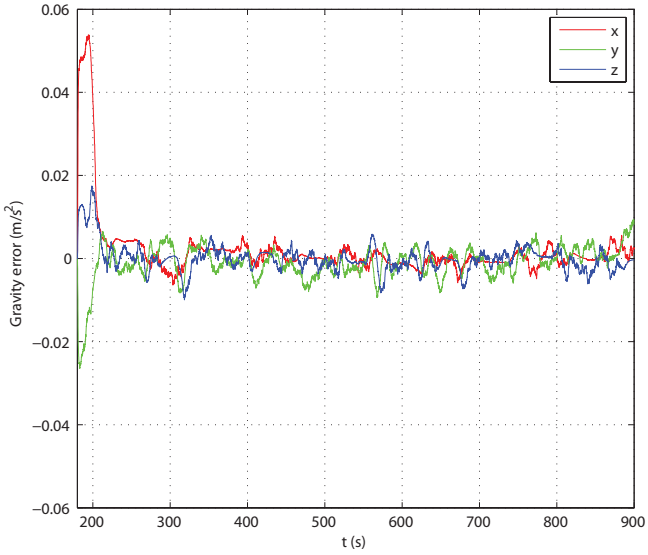

Fig. 7. Evolution of the gravity error

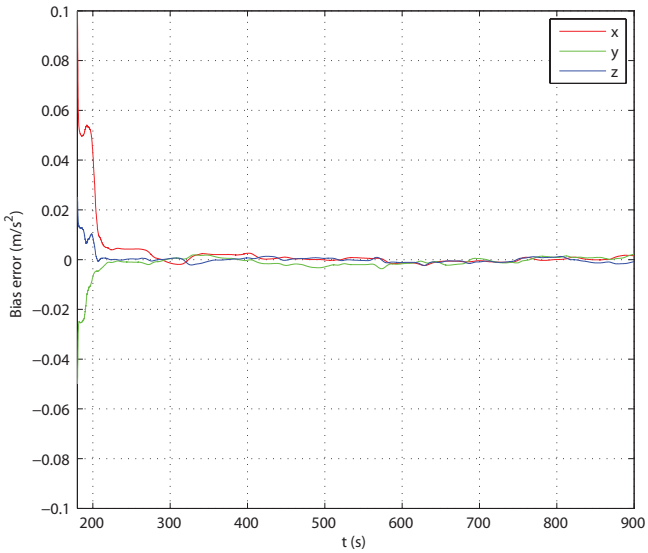

Fig. 8. Evolution of the bias error

and systems. This table, presented in Fig. 9, was used to generate the desired calibration trajectories and provide the required ground truth signals. The angular resolution of the MRT is $0.000025\,^{\circ}$. The accelerometer that was employed is presented in Fig. 10. It is a Silicon Design Inc. triaxial analog accelerometer [22], sampled at 100 Hz using three Texas Instruments ADS1210, which are directly connected to a microcontroller board built around the Phillips XAS3 16-bit microcontroller with CAN (Controller Area Network) Bus interface [23]. The ADS1210 is a high precision, wide dynamic range, delta-sigma analog-to-digital converter (ADC), with 24-bit resolution, and operates from a single +5V supply. The ADS1210 differential inputs are ideal for direct connection to transducers, guaranteeing 20-bits of effective resolution, which is a suitable accuracy for the inertial sensor used in the present application. Finally, a PC104 board, connected to the CAN Bus, logs the data in a solid state disk for post-testing analysis. The table top is autonomous in terms of power and logging capabilities.

Fig. 9. Experimental setup mounted on the Ideal Aerosmith calibration table

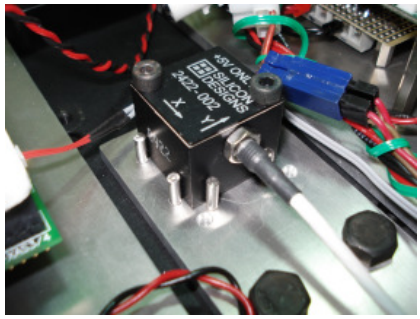

Fig. 10. Accelerometer

B. Dynamic Accelerometer Calibration

The accelerometer unit previously introduced was subject to several tests, taken on different days and in different conditions. The calibration results show that the scale and cross factors, as well as the quadratic coefficient, do not change significantly between tests, which validates the calibration of the accelerometer prior to its usage in navigation systems. However, the bias estimates resulting from the calibration test proposed in Section III change greatly between tests, including tests where the accelerometer power was never turned off. This evidences that dynamic bias estimation is essential for this type of sensor.

The estimated parameters, which were used to correct the acceleration measurements afterwards during dynamic bias and gravity estimation, were

$$\mathbf{F}^{-1} = \begin{bmatrix} 0.9946 & 0.0037 & -0.0061 \\ -0.0091 & 0.9998 & 0.0079 \\ -0.0071 & -0.0186 & 1.0047 \end{bmatrix},$$

$$\mathbf{b}' = \begin{bmatrix} -0.7368 \\ -0.2803 \\ 0.3995 \end{bmatrix} \ (\mathrm{m/s^2}),$$

and

$$\mathbf{F}_2 = 10^{-4}\mathrm{diag}\left(-2.362, 1.055, 3.666\right).$$

These are all within the specifications provided by the manufacturer.

Figure 11 presents the error between the corrected accelerometer measurements at static positions and the expected measurements, which are due only to the acceleration of gravity. It is possible to observe that, even after accelerometer calibration, the mean of the error at each position is not always zero. This is due not only to higher-order nonlinearities but also to the time-varying nature of the parameters. There exist some positions at which the standard deviation of the error is much higher. This is not due to the accelerometer but to the calibration table, which exhibited some oscillations at some positions. Finally, a vibration was detected in the outer axis of the calibration table around 11Hz, which is most likely a natural resonance frequency of the body. That also contributes to the increased standard deviation of the error, and that is not present in real applications. Interestingly enough, both the oscillations and the vibrations of the table are so small that a slightly lower grade accelerometer is unable to detect them.

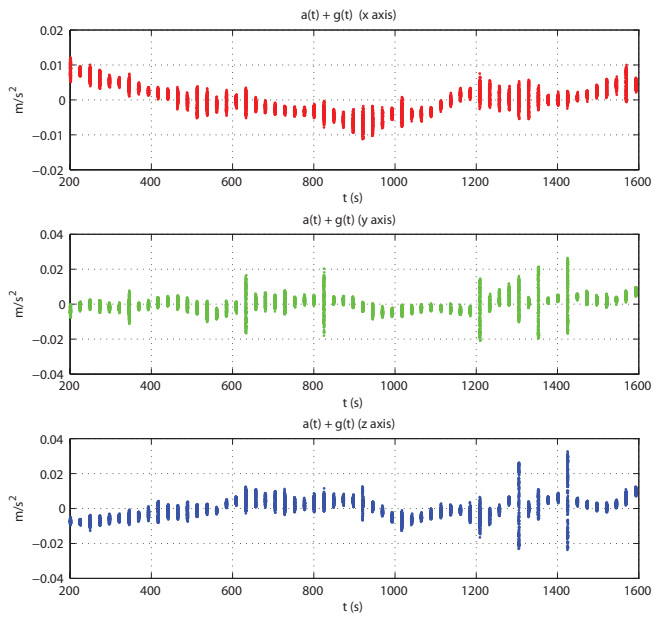

Fig. 11. Error of the accelerometer measurements after calibration correction

C. Dynamic Bias and Gravity Estimation

The experimental results relative to dynamic bias and gravity estimation are presented in this section. The evolution of the attitude is the same as the one presented in Section V-B, so that the results are comparable. The filter parameters, sampling rate, and initial estimates are also the same. Notice that, with this trajectory, the system dynamics for on-line dynamic bias and gravity estimation are uniformly completely observable, so that the Kalman filter error dynamics are globally asymptotically stable.

The evolution of the gravity and bias estimates are depicted in Figs. 12 and 13, respectively. The similarities between

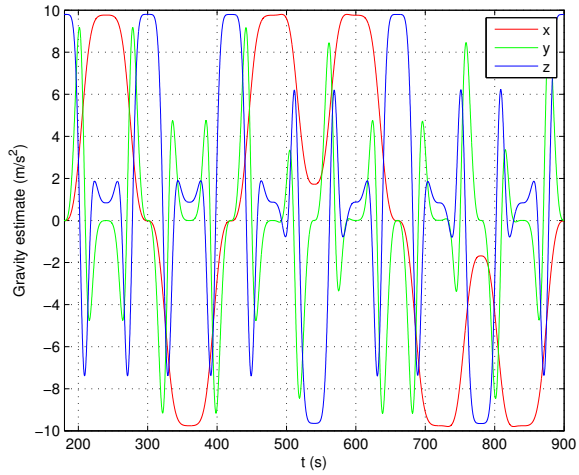

Fig. 12. Evolution of the gravity estimate (in body-fixed coordinates)

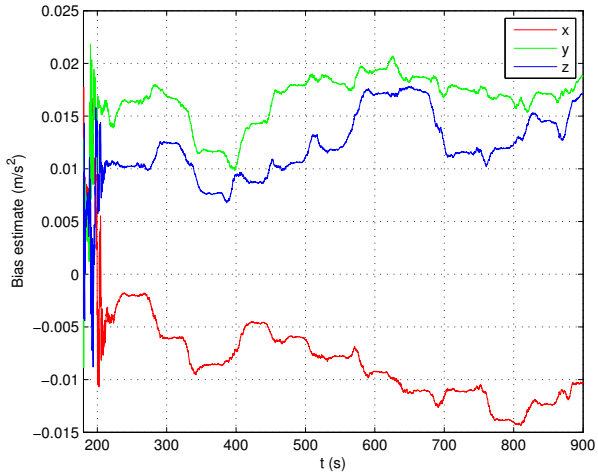

Fig. 13. Evolution of the bias estimate

Fig. 12 and Fig. 4 evidence that the experimental results follow closely the simulation results. It is possible to observe that the filter keeps very good tracking of the acceleration of gravity, which is essential for attitude estimation purposes in navigation systems. It is also possible to see the time-varying nature of the bias.

Comparing the level of the accelerometer error at rest (after calibration), presented in Fig. 11, with the magnitude of the bias estimate, depicted in Fig. 13, they seem about the same for this particular unit. Nevertheless, it is important to remark that it does not render the bias estimation process useless. Indeed, any acceleration bias that is not compensated for in a navigation system leads to the degradation of the system performance, particularly due to the double integration that

relates acceleration and position quantities. Moreover, it is important to stress that the bias estimate is only small in this case because the accelerometer unit had been calibrated and therefore the bias was partially compensated for, as shown in Section VI-B. Had this not been the case and the bias estimate would be very large when compared to the accelerometer noise.

In order to better assess the performance of the filter, the evolution of the errors of the linear velocity and gravity acceleration are depicted in Figs. 14 and 15, respectively. Clearly, the mean errors converge to zero. Moreover, the error on the gravity stays well below the noise of the accelerometer, which evidences very good filtering performance.

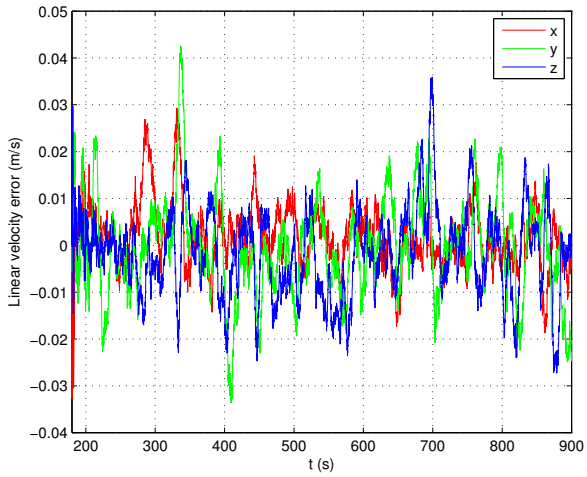

Fig. 14. Evolution of the linear velocity error

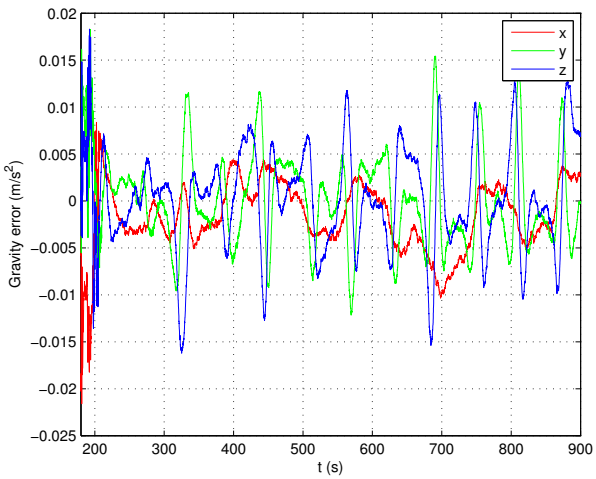

Fig. 15. Evolution of the gravity error

VII. Conclusions

Tri-axial accelerometers are key elements in a great variety of applications and, in particular, in navigation systems. Nonidealities such as scale factors, cross coupling, and bias, affect the output of this sensor, leading, in general, to prohibitive errors, particularly for sensitive and high-performance navigation systems. This justifies off-line calibration as a method to overcome these nonidealities. On the other hand, these coefficients are often time-varying, which renders off-line calibration less effective and calls for dynamic parameter estimation. This paper presented a calibration technique for a triaxial accelerometer and a novel dynamic filtering solution for the bias, which also accounts explicitly for the estimation of the gravity in body-fixed coordinates. Simulation results were shown that evidenced the expectable performance of the proposed algorithms. Finally, a low-cost accelerometer unit was calibrated and the dynamic bias and gravity estimation evaluated experimentally. In the tests a Motion Rate Table was employed that provided ground truth signals for performance evaluation purposes, both for off-line calibration and dynamic bias and gravity estimation, and that allowed to conclude the excellent performance of the proposed solutions. Future work will consist in the inclusion of the proposed dynamic estimation solution in future navigation systems, previously adjusted with the calibration algorithm presented in the paper.

Acknowledgments

The authors gratefully acknowledge the expertise and contributions of Luís Sebastião during the mounting process of the Ideal Aerosmith Calibration Table and the help with the delogging software provided by André Oliveira.

References

[1] R. Mahony, T. Hamel, and J.-M. Pflimlin, "Nonlinear Complementary Filters on the Special Orthogonal Group," *IEEE Transactions on Automatic Control*, vol. 53, no. 5, pp. 1203–1218, Jun. 2008.

[2] P. Batista, C. Silvestre, and P. Oliveira, "Sensor-based Complementary Globally Asymptotically Stable Filters for Attitude Estimation," in *Proceedings of the 48th IEEE Conference on Decision and Control*, Shanghai, China, Dec. 2009, pp. 7563–7568.

[3] ——, "Position and Velocity Optimal Sensor-based Navigation Filters for UAVs," in *Proceedings of the 2009 American Control Conference*, Saint Louis, USA, Jun. 2009, pp. 5404–5409.

[4] "IEEE Recommended Practice for Precision Centrifuge Testing of Linear Accelerometers," IEEE Std. 836, 1991.

[5] D. Titterton and J. Weston, *Strapdown Inertial Navigation Systems*. The Institution of Electrical Engineers, 2004.

[6] M. Kayton and W. Fried, *Avionics Navigation Systems*. John Wiley & Sons, Inc., 2003.

[7] R. Rogers, *Applied Mathematics in Integrated Navigation Systems*. AIAA, 2003.

[8] B. Barshan and H. Durrant-Whyte, "Inertial navigation systems for mobile robots," *IEEE Transactions on Robotics and Automation*, vol. 11, no. 3, pp. 328–342, Jun. 1995.

[9] M. Grewal, V. Henderson, and R. Miyasako, "Application of Kalman Filtering to the Calibration and Alignment of Inertial Navigation Systems," *IEEE Transactions on Automatic Control*, vol. 36, no. 1, pp. 4–13, Jan. 1991.

[10] E. Nebot and H. Durrant-Whyte, "Initial calibration and alignment of an inertial navigation," in *Proceedings of the 4th Annual Conference on Mechatronics and Machine Vision in Practice*, Toowoomba, Australia, Sep 1997, pp. 175–180.

[11] M. Stakkeland, G. Prytz, W. Booij, and S. Pedersen, "Characterization of Accelerometers Using Nonlinear Kalman Filters and Position Feedback," *IEEE Transactions on Instrumentation and Measurement*, vol. 56, no. 6, pp. 2698–2704, Dec. 2007.

[12] E. Renk, W. Collins, M. Rizzo, F. Lee, and D. Bernstein, "Optimization-based calibration of a triaxial accelerometer-magnetometer," in *Proceedings of the 2005 American Control Conference*, vol. 3, Portland, OR, USA, June 2005, pp. 1957–1962.

[13] N. Dumas, F. Azais, F. Mailly, A. Richardson, and P. Nouet, "A novel method for test and calibration of capacitive accelerometers with a fully electrical setup," in *11th IEEE Workshop on Design and Diagnostics of Electronic Circuits and Systems*, Bratislava, Slovakia, April 2008.

[14] J. Hall and R. Williams, "Case study: Inertial measurement unit calibration platform," *Journal Robotic Systems*, vol. 17, no. 11, pp. 623–632, 2000.

[15] P. Walter, "The History of the Accelerometer," *Sound and Vibration*, pp. 84–92, 2007.

[16] A. Kelly, "Modern Inertial and Satellite Navigation Systems," Robotics Institute, Carnegie Mellon University, Pittsburgh, PA, Tech. Rep. CMU-RI-TR-94-15, May 1994.

[17] Department of Defense World Geodetic System, "Its Definition and Relationships With Local Geodetic Systems," Tech. Rep. NIMA TR8350.2, 1984.

[18] P. Batista, C. Silvestre, and P. Oliveira, "Necessary and sufficient conditions for the observability of linear motion quantities in strapdown navigation systems," in *Proceedings of the 2009 American Control Conference*, Saint Louis, MO, USA, Jun. 2009.

[19] R. Kalman and R. Bucy, "New Results in Linear Filtering and Prediction Theory," *Journal of Basic Eng., Transactions ASME, Series D*, vol. 83, no. 3, pp. 95–108, Mar. 1961.

[20] A. Gelb (Ed), *Applied Optimal Filtering*. The MIT Press, 1974.

[21] Ideal Aerosmith, Inc., "2103HT Multi-Axis Table Data Sheet, Rev C," http://www.ideal-aerosmith.com/, 2006.

[22] Silicon Designs, Inc., "TRIAXIAL ANALOG ACCELEROMETER MODULE, Model 2422," www.silicondesigns.com, 2007.

[23] Bosch, R., "CAN specification version 2.0." Tech. Rep., 1991.